SINGULARITY AVOIDANCE ALGORITHMS FOR SPACECRAFT ATTITUDE CONTROL USING SINGLE GIMBAL CONTROL MOMENT GYROSCOPES

Benny Susanto Budiman
University Undergraduate Fellow, 1990–91
Texas A&M University
Department of Aerospace Engineering

APPROVED:

Fellows Advisor Srinivas R. Vadali

Honors Program Director

ABSTRACT

Singularity Avoidance Algorithms for Spacecraft
Attitude Control using Single Gimbal Control Moment Gyroscopes

Benny Susanto Budiman
University Undergraduate Fellow, 1990–1991
Texas A&M University
Department of Aerospace Engineering

Fellows Advisor: Dr. Srinivas R. Vadali

Single gimbal control moment gyroscopes are attractive actuators for spacecraft attitude control systems. However, intrinsic kinematic singularities preclude torque generation along certain directions and lead to loss of three-axis control of the spacecraft. Kinematic singularities also exist in robotic manipulator systems which are mechanical analogs of the single gimbal control moment gyroscope systems. In robotic manipulator systems, kinematic singularities preclude end-effector motions in singular directions. An algorithm is proposed to avoid singularities in control moment gyroscope systems. The proposed algorithm is based on the extended Jacobian, used to solve singularity avoidance problem in the robotic manipulator system, and the null motion avoidance algorithms. The current algorithm has been shown to avoid internal kinematic singularities when applied to spacecraft maneuver problems. Feedback torque requests are generated using control laws based on the Liapunov's stability theory.

ACKNOWLEDGMENT

The author wishes to express his sincere appreciation to his Fellows advisor, Dr. S. R. Vadali, who has given continuous guidance and encouragement throughout the Fellows year 1990-1991. The author would like to thank the University Honors Office, particularly Dr. Knobel and Ms. Cowley, for the support and opportunity to participate in the University Undergraduate Fellows program.

TABLE OF CONTENTS

LIST OF FIGURES

I. INTRODUCTION

Single gimbal control moment gyroscopes (SCMGs) are angular momentum transfer devices used as actuators in spacecraft attitude control systems. The SCMGs have significant advantages over other actuators: thrusters, reaction wheels and double gimbal control moment gyroscopes (DCMGs). Unlike the thrusters, the SCMGs do not have expendable propellant which may contaminate the sensitive space environment and can be used in rapid and precision maneuvers. The SCMGs have constant motor speed, unlike the reaction wheels, which is very unlikely to excite vibrational modes of the spacecraft structure. The SCMGs have simpler mechanical configurations than the DCMGs, and can provide torque amplification.

Despite the advantages, the SCMG systems have analytical difficulties: the existence of singular gimbal configurations (kinematic singularities) which occur when the output torque of each gimbal is perpendicular to the singular direction in space, and hence preclude torque generation in certain (singular) directions. In the neighborhood of singular states, high gimbal rates are necessary to generate the requested torque to perform the maneuver. However, hardware limits on gimbal rates further preclude torque generation in the neighborhood of singularities. Thus singularities lead to loss of three-axis control of the spacecraft and further, keep the SCMG system from being fully utilized by the attitude control systems. Therefore, development of a control algorithm is necessary to avoid kinematic singularities.

A mechanical analogy exists between the SCMG and the robotic manipulator (RM) systems[1,2]. Singular configurations (kinematic singularities) exist in both systems. The RM systems are slightly more complicated than the SCMG, as they also encounter repeatability and obstacle avoidance problems. Pertinent works in the RM

systems include the augmented Jacobian technique by Baillieul[3] and the optimal path planning problem by Mayorga and Wong[4]. Nenchev[5] summarizes similar works in the RM systems.

Previous works on singularity avoidance issues include the fundamental work on identification and classification of different types of singularities by Margulies and Aubrun[1], null motion avoidance algorithms by Cornick[6], singularity robust (SR) inverse by Nakamura and Hanafusa[7] (used for solving the robotic manipulator steering problem and shown to be applicable to the SCMG steering problem by Bedrossian[2]), and preferred initial gimbal angles by Vadali et al[8]. Most of the algorithms have not been able to avoid internal kinematic singularities completely.

This thesis addresses the issue of avoiding kinematic singularities in the SCMG systems and the application of the avoidance algorithm in spacecraft attitude control systems. The thesis also reviews recent advances in singularity avoidance problem for the RM systems and applies some of the methods, indirectly, to avoiding kinematic singularities in the SCMG systems. This thesis is divided into four major parts: (a) Fundamental concepts of the SCMG and RM systems, (b) Singularity analysis and existing avoidance algorithms in the SCMG and RM systems, (c) Development of the proposed singularity avoidance algorithm, (d) Application of the proposed algorithm for spacecraft attitude control using SCMGs.

II. FUNDAMENTAL CONCEPTS

1. Single Gimbal Control Moment Gyroscope System

A SCMG system consists of a number of flywheels arranged in a certain configuration. Each flywheel spins at a constant rate about an axis (momentum axis) which is gimballed to allow its angular momentum to rotate on the plane of rotation. Each gimbal is free to rotate about the gimbal axis which is normal to the plane of rotation. The positive angular displacement is defined by the gimbal axis rotation.

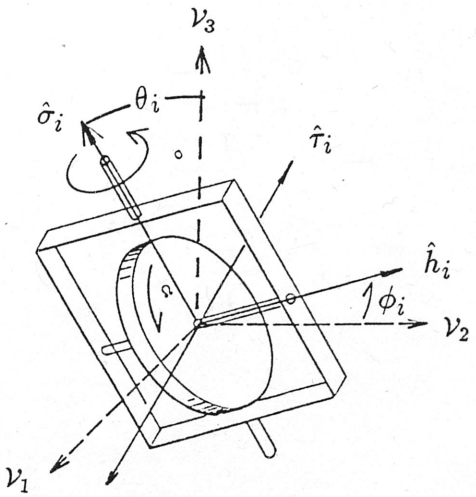

Figure 1 The ith SCMG reference frame and its orientation with respect to the spacecraft frame.

Each gimbal reference frame, $\mathcal{G}_i$, is defined by an orthonormal basis $\{-\hat{\tau}_i\ \hat{h}_i\ \hat{\sigma}_i\}$ where $\hat{\sigma}_i$ denotes a unit vector along its gimbal axis, $\hat{h}_i$ denotes a unit vector along its momentum axis, and $\hat{\tau}_i$ is defined by the formula $\hat{\tau}_i = \hat{\sigma}_i \times \hat{h}_i$ (Fig.1). The relative orientation of each gimbal reference frame with respect to the spacecraft frame $\mathcal{V}$ can be represented as

$$\mathbf{C}_{\mathcal{V}\mathcal{G}_i} = \begin{pmatrix} c\phi_i c\theta_i c\sigma_i - s\phi_i s\sigma_i & -c\phi_i c\theta_i s\sigma_i - s\phi_i c\sigma_i & c\phi_i s\theta_i \\ s\phi_i c\theta_i c\sigma_i + c\phi_i s\sigma_i & -s\phi_i c\theta_i s\sigma_i + c\phi_i c\sigma_i & s\phi_i s\theta_i \\ -s\theta_i c\sigma_i & s\theta_i s\sigma_i & c\theta_i \end{pmatrix} \tag{2.1}$$

where ϕ_i, θ_i, and σ_i are the 3-2-3 set of Euler angles depicted in Fig.1; and $c\sigma_i \triangleq \cos\sigma_i$, $s\sigma_i \triangleq \sin\sigma_i$, etc.

The angular momentum vector of each gimbal is fixed in the corresponding gimbal frame and is given by $\underline{h}_{\mathcal{G}_i} = \{0\ h_i\ 0\}^{\mathrm{T}}$. The angular momentum can be expressed in the spacecraft frame as

$$\underline{h}_{\mathcal{V}_i} = \mathbf{C}_{\mathcal{V}\mathcal{G}_i}\underline{h}_{\mathcal{G}_i} \tag{2.2}$$

Each gimbal frame rotates about its gimbal axis with an angular velocity of $\underline{\dot{\sigma}}_{\mathcal{G}_i} = \{0\ 0\ \dot{\sigma}_i\}^{\mathrm{T}}$ in the gimbal frame. Thus the output torque of each gimbal can be represented as

$$\underline{\tau}_{\mathcal{V}_i} = \mathbf{C}_{\mathcal{V}\mathcal{G}_i}\tilde{\dot{\sigma}}_i\underline{h}_{\mathcal{G}_i} \tag{2.3}$$

where

$$\tilde{\dot{\sigma}}_i \triangleq \begin{pmatrix} 0 & -\dot{\sigma}_i & 0 \\ \dot{\sigma}_i & 0 & 0 \\ 0 & 0 & 0 \end{pmatrix}$$

represents the skew symmetric cross product matrix of $\underline{\dot{\sigma}}_i$. In deriving Eq.(2.3), the terms containing the inertia matrix of the flywheels have been dropped because their effects are negligible compared to those of the terms in Eq.(2.3) as justified in Ref.10.

A SCMG system generally consists of n flywheels, thus the total momentum of the system is given by

$$\underline{h}_{\mathrm{CMG},\mathcal{V}} = \sum_{i=1}^{n} \mathbf{C}_{\mathcal{V}\mathcal{G}_i}\underline{h}_{\mathcal{G}_i} \tag{2.4}$$

and the total output torque of the system can be expressed as

$$\underline{\tau}_{\mathrm{CMG},\mathcal{V}} = \sum_{i=1}^{n} \mathbf{C}_{\mathcal{V}\mathcal{G}_i}\tilde{\dot{\sigma}}_i\underline{h}_{\mathcal{G}_i} \tag{2.5}$$

This thesis focuses on a system which consists of four gimbals arranged in a pyramid configuration characterized with $\phi_i = (i-1)\cdot 90^\circ$, $\theta_i = \theta = 54.74^\circ$, and $h_i = h$ as shown in Fig.2. Thus Eq.(2.5) can be explicitly expressed as

$$\underline{\tau}_{\mathrm{CMG},\nu} = \mathbf{J}\dot{\underline{\sigma}} \tag{2.5b}$$

where

$$\mathbf{J} = h\begin{pmatrix} -\mathrm{c}\theta\mathrm{c}\sigma_1 & \mathrm{s}\sigma_2 & \mathrm{c}\theta\mathrm{c}\sigma_3 & -\mathrm{s}\sigma_4 \\ -\mathrm{s}\sigma_1 & -\mathrm{c}\theta\mathrm{c}\sigma_2 & \mathrm{s}\sigma_3 & \mathrm{c}\theta\mathrm{c}\sigma_4 \\ \mathrm{s}\theta\mathrm{c}\sigma_1 & \mathrm{s}\theta\mathrm{c}\sigma_2 & \mathrm{s}\theta\mathrm{c}\sigma_3 & \mathrm{s}\theta\mathrm{c}\sigma_4 \end{pmatrix}$$

is usually referred to as the *Jacobian* of $\underline{h}_{\mathrm{CMG},\nu}$ expressed as

$$\mathbf{J} = \frac{\partial}{\partial \underline{\sigma}}\underline{h}(\sigma)_{\mathrm{CMG},\nu}$$

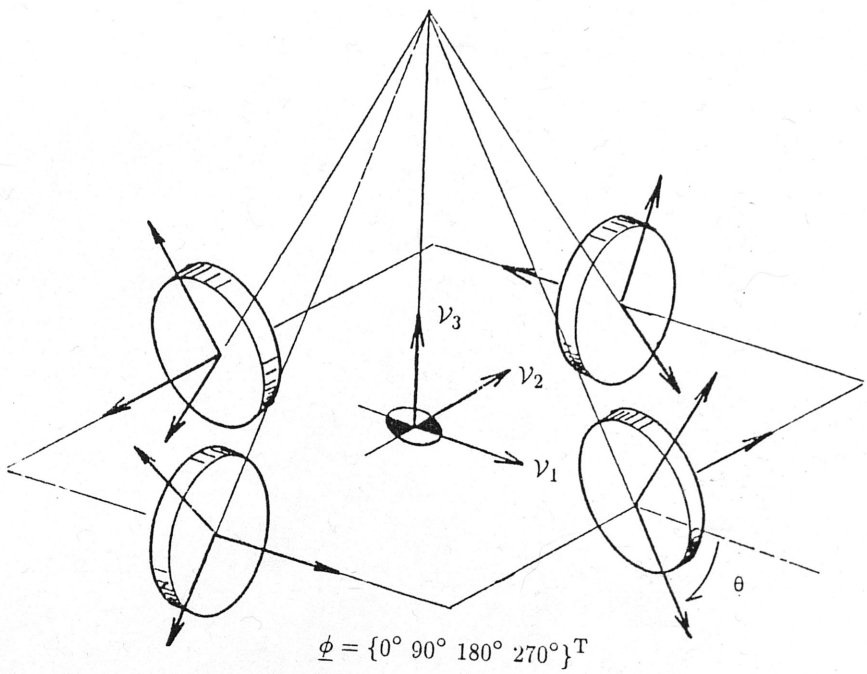

Figure 2 Pyramid type SCMG configuration, $\underline{\sigma} = \underline{0}$.

As actuators, the SCMGs have to generate some prescribed torques to maneuver the spacecraft. This task is accomplished by rotating the angular momentum vector of each gimbal at certain rates of gimbal rotation. The gimbal rates are obtained by

solving Eq.(2.5b), an underdetermined system of equations, using the pseudoinverse of $\mathbf{J}$ given by[1,9]

$$\mathbf{J}^{+} = \mathbf{J}^{\mathrm{T}}\left(\mathbf{J}\mathbf{J}^{\mathrm{T}}\right)^{-1} \tag{2.6}$$

2. Robotic Manipulator System, A Mechanical Analog

A robotic manipulator consists of numerous linkages connected by joints. The outer-most linkage moves objects in prescribed trajectories and is referred to as the end-effector. As described in [4] and [7], end-effector trajectories are analogous to total angular momentum of the SCMG system. For simplicity, this section discusses only the planar two degrees of freedom RM systems with one degree of redundancy.

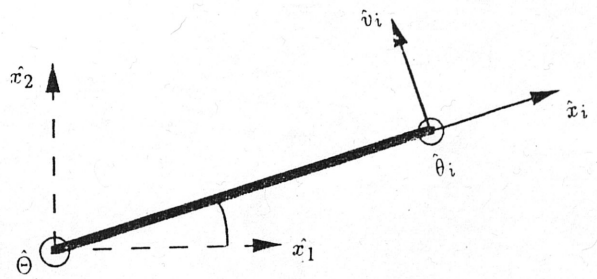

Figure 3 The ith linkage reference frame in a robotic manipulator system.

Each linkage reference frame, $\mathcal{L}_i$, is defined by an orthonormal basis $\{\hat{x}_i\ \hat{v}_i\ \hat{\theta}_i\}$ where $\hat{l}_i$ denotes a unit vector along the linkage, $\hat{v}_i$ denotes a unit vector perpendicular to $\hat{v}_i$, and $\hat{\theta}_i$ is defined by $\hat{\theta}_i = \hat{l}_i \times \hat{v}_i$ (Fig.3). In a planar 2-DOF manipulator, $\mathcal{L}_i$ is constrained to rotate about its origin in the l_i-v_i plane with respect to the fixed frame $\mathcal{X}$. The relative orientation of $\mathcal{L}_i$ with respect to $\mathcal{X}$ can be represented as

$$\mathbf{C}_{\mathcal{X}\mathcal{L}_i} = \begin{pmatrix} \mathrm{c}\theta_i & -\mathrm{s}\theta_i & 0 \\ \mathrm{s}\theta_i & \mathrm{c}\theta_i & 0 \\ 0 & 0 & 1 \end{pmatrix} \tag{2.7}$$

Each linkage has a fixed length L_i and is represented as a position vector $\underline{x}_{\mathcal{L}_i} = \{L_i\ 0\ 0\}^{\mathrm{T}}$, which can be expressed in $\mathcal{X}$ as

$$\underline{x}_{\mathcal{X}_i} = \mathbf{C}_{\mathcal{X}\mathcal{L}_i}\underline{x}_{\mathcal{L}_i} \tag{2.8}$$

Each linkage frame rotates about $\hat{\theta}_i$ with an angular velocity of $\underline{\dot{\theta}}_{\mathcal{L}_i} = \{0\ 0\ \dot{\theta}_i\}^{\mathrm{T}}$. Thus the end velocity of each linkage with respect to $\mathcal{X}$ can be written as

$$\underline{v}_{\mathcal{X}_i} = \mathbf{C}_{\mathcal{X}\mathcal{L}_i}\tilde{\dot{\theta}}_i\underline{x}_{\mathcal{L}_i} \tag{2.9}$$

where

$$\tilde{\dot{\theta}}_i \triangleq \begin{pmatrix} 0 & -\dot{\theta}_i & 0 \\ \dot{\theta}_i & 0 & 0 \\ 0 & 0 & 0 \end{pmatrix}$$

represents the skew symmetric cross product matrix of $\underline{\dot{\theta}}_i$.

A RM system usually has n linkages, thus the position of the end-effector in $\mathcal{X}$ is given by

$$\underline{x}_{\mathcal{X}} = \sum_{i=1}^{n} \mathbf{C}_{\mathcal{X}\mathcal{L}_i}\underline{x}_{\mathcal{L}_i} \tag{2.10}$$

and the velocity of the end-effector can be expressed as

$$\underline{v}_{\mathcal{X}} = \sum_{i=1}^{n} \mathbf{C}_{\mathcal{X}\mathcal{L}_i}\tilde{\dot{\theta}}_i\underline{x}_{\mathcal{L}_i} \tag{2.11}$$

For planar two degrees of freedom RM systems with one degree of redundancy ($n = 3$) and $L_i = L$, Eq.(2.11) can be explicitly rewritten as

$$\underline{v}_{\mathcal{X}} = \mathbf{J}\underline{\dot{\theta}} \tag{2.11b}$$

where

$$\mathbf{J} = L\begin{pmatrix} -\mathrm{s}\theta_1 & -\mathrm{s}\theta_2 & -\mathrm{s}\theta_3 \\ \mathrm{c}\theta_1 & \mathrm{c}\theta_2 & \mathrm{c}\theta_3 \end{pmatrix}$$

is the Jacobian of $\underline{x}_{\mathcal{X}}$ given by

$$\mathbf{J} = \frac{\partial}{\partial\underline{\theta}}\underline{x}(\theta)_{\mathcal{X}}$$

The joint rates are obtained by solving Eq.(2.11b) using the pseudoinverse of the Jacobian, given in Eq.(2.6).

III. SINGULARITY ANALYSIS

1. Introduction

In general, Eqs.(2.4) and (2.10) are nonlinear and pointwise vector-valued mappings $f : \Re^n \rightarrow \Re^m$, from the physical (gimbal or linkage) space to the operational (momentum or trajectory) space, respectively. Note that $(\underline{\sigma}, \underline{\theta}) \in \Re^n$ and $(\underline{h}_{CMG,\nu}, \underline{x}_x) \in \Re^m$. Closed-form analytical inverses (solutions) of the mappings cannot be obtained, hence differential relationships are used to solve for the gimbal/linkage motion from a given momentum or trajectory of the end-effector, such as Eqs.(2.5) and (2.11). This type of solution is often referred to as the *resolved motion rate control* [11].

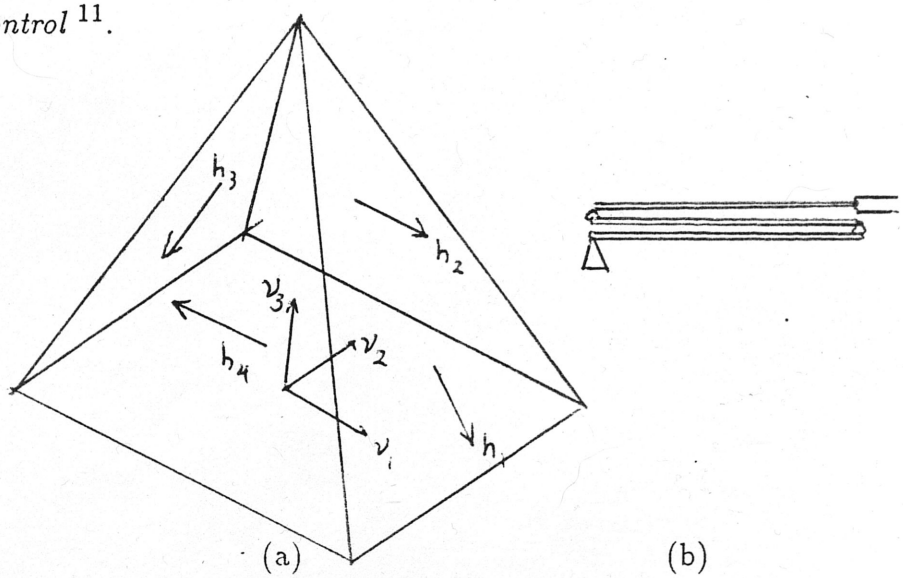

Figure 4 Internal gimbal (a) and linkage (b) singular configurations. In a SCMG system, torque cannot be produced along the $\mathcal{V}_1$ axis, whereas in a RM system, motion of the end-effector is not possible in the singular direction.

Singular gimbal/linkage configurations are defined mathematically as the configurations of gimbal angles (linkage positions) which result in a rank-deficient Jacobian

matrix of the systems (rank($\mathbf{J}$) is less than the number of degrees of freedom (m) of the systems). Physically, singular configurations in a SCMG system occur when the output torque of each flywheel (gimbal) is perpendicular to the singular direction, or when the angular momentum of each gimbal is maximally/minimally projected onto the singular direction. Thus no torque can be generated in this direction. In a RM system, singular configurations occur when the end velocity of each linkage is perpendicular to the singular direction, or the position vector of each linkage is maximally/minimally projected onto the singular direction. Thus motions of the end-effector are not possible along the singular direction. Fig.4 shows examples of internal singular configurations for (a) the SCMG and (b) the RM systems.

2. Identification of Singularities

This section discusses the singular gimbal configurations for any given direction in $\Re^m$.The purpose is to illustrate that for any given direction in space, a system of n SCMGs has as many as 2^n singular gimbal configurations. The statement also holds true for a RM system with n linkages.

Any direction in space can be represented as (Fig.5)

$$\underline{\hat{u}} = \mathrm{c}\theta_1\mathrm{c}\theta_2\underline{\hat{h}}_1 + \mathrm{c}\theta_1\mathrm{s}\theta_2\underline{\hat{h}}_2 + \mathrm{s}\theta_1\underline{\hat{h}}_3 \tag{3.1}$$

and the projection of any vector $\underline{v}$ onto $\underline{\hat{u}}$ is defined as

$$\mathcal{P} \triangleq \underline{v} \cdot \underline{\hat{u}} \tag{3.2}$$

By definition, singular gimbal ($\underline{\sigma}^s$) or linkage ($\underline{\theta}^s$) configurations occur when the angular momentum of each gimbal or the position vector of each linkage is maximally/minimally projected onto the singular direction. Hence the necessary and

sufficient conditions are:

$$\left(\frac{\partial \mathcal{P}}{\partial \underline{\sigma}_i}\right)_{\text{CMG}} = 0 \quad \text{and} \quad \left(\frac{\partial^2 \mathcal{P}}{\partial \underline{\sigma}_i^2}\right)_{\text{CMG}} < 0, \qquad i = 1, 2, \ldots, n \tag{3.3a}$$

for a SCMG system ($\mathcal{P} = \underline{h}_{\text{CMG},\nu_i} \cdot \hat{\underline{u}}$), or

$$\left(\frac{\partial \mathcal{P}}{\partial \underline{\theta}_i}\right)_{\text{RM}} = 0 \quad \text{and} \quad \left(\frac{\partial^2 \mathcal{P}}{\partial \underline{\theta}_i^2}\right)_{\text{RM}} < 0, \qquad i = 1, 2, \ldots, n \tag{3.3b}$$

for a RM system ($\mathcal{P} = \underline{x}_{\chi_i} \cdot \hat{\underline{u}}$).

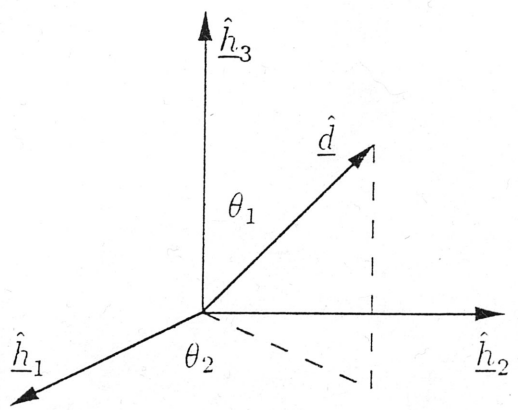

Figure 5 Any direction in $\Re^3$ can be represented by two parameters or generalized coordinates.

Also, by definition, singular gimbal ($\underline{\sigma}^s$), or linkage ($\underline{\theta}^s$), configurations occur when the output torque of each gimbal ($\underline{\tau}_i$), or the end velocity of each linkage ($\underline{v}_i$), is perpendicular to the singular direction, or mathematically

$$\hat{\tau}_i \cdot \hat{\underline{u}} = 0 \tag{3.4a}$$

for a SCMG system, or

$$\hat{v}_i \cdot \hat{\underline{u}} = 0 \tag{3.4b}$$

for a RM system.

Because $\hat{\tau}_i(\hat{v}_i)$ must be orthogonal to $\hat{\sigma}_i$ $(\hat{\theta}_i)$, a necessary and sufficient condition for Eqs.(3.4a,b) is

$$\hat{\tau}_i = \pm \frac{\hat{\sigma}_i \times \underline{\hat{u}}}{|\hat{\sigma}_i \times \underline{\hat{u}}|}, \quad \underline{\hat{u}} \neq \pm \hat{\sigma}_i \tag{3.5a}$$

for a SCMG system, or

$$\hat{v}_i = \pm \frac{\hat{\theta}_i \times \underline{\hat{u}}}{|\hat{\theta}_i \times \underline{\hat{u}}|}, \quad \underline{\hat{u}} \neq \pm \hat{\theta}_i \tag{3.5b}$$

for a RM system.

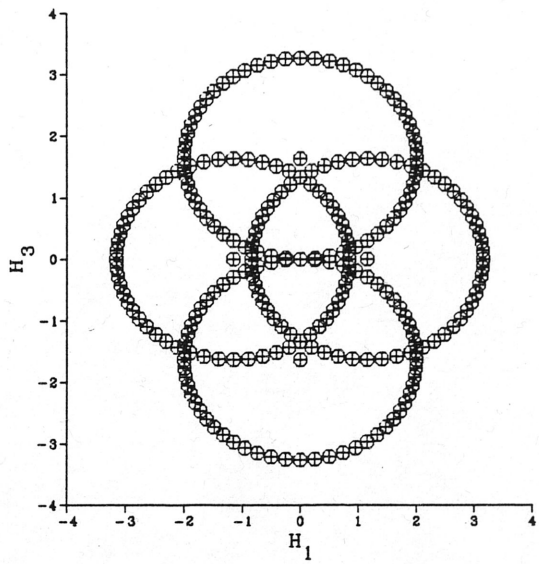

Figure 6 The projection of singular momentum envelope onto the h_1-h_3 plane.

Since $\hat{h}_i = \hat{\tau}_i \times \hat{\sigma}_i$ $(\hat{x}_i = \hat{v}_i \times \hat{\theta}_i)$, the singularity condition for $\hat{h}_{\nu_i}$ $(\hat{x}_{\chi_i})$ can be written as

$$\hat{h}^s_{\nu_i}(\underline{\hat{u}}) = \pm \frac{\hat{\sigma} \times \underline{\hat{u}}}{|\hat{\sigma} \times \underline{\hat{u}}|} \times \hat{\sigma} \tag{3.6a}$$

for a SCMG system, or

$$\hat{l}^s_{\chi_i}(\underline{\hat{u}}) = \pm \frac{\hat{\theta} \times \underline{\hat{u}}}{|\hat{\theta} \times \underline{\hat{u}}|} \times \hat{\theta} \tag{3.6b}$$

for a RM system.

The signs (± 1) in Eqs.(3.5–6) result in 2^n sign patterns; each pattern corresponds to one singular configuration. Hence, for any given direction in $\Re^m$, there are 2^n singular gimbal (linkage) configurations. For a system of four SCMGs, the patterns can be tabulated as follows:

+	−	+	+	+	−	−	−	+	+	+	−	−	−	+	−
+	+	−	+	+	−	+	+	−	−	+	−	−	+	−	−
+	+	+	−	+	+	−	+	−	+	−	−	+	−	−	−
+	+	+	+	−	+	+	−	+	−	−	+	−	−	−	−
0	1	2	3	4	5	6	7	8	9	10	11	12	13	14	15

The projection of singular momentum envelope onto the h_1-h_3 plane is depicted in Fig.6. Similar sign patterns and singular trajectory envelope can also be generated for a RM system in the same fashion.

3. Classification of Singularities

Kinematic singularities are classified according to their loci in the total SCMG angular momentum envelope (RM trajectory envelope)[1,2]. Kinematic singularities can be classified as: (a) Surface or saturation singularities and (b) Internal singularities (elliptic and hyperbolic).

Saturation singularities correspond to gimbal (linkage) configurations which result in maximum projection of gimbal momentum capacity (end-effector trajectory) along certain (singular) directions. This type of singularities corresponds to the maximum physical momentum (trajectory) capability of the SCMG (RM) systems. In spacecraft application, the saturation singular configurations cannot be avoided using steering algorithm alone. A momentum management procedure (Vadali and Oh[12]) must be used to keep the SCMG momentum within the momentum envelope of the system.

Internal singularities may be escapable using null motion. Bedrossian[2] presents an approach to examine the behavior of a SCMG (RM) system using null motion near a singular configuration. The null motion test is determined by[2]

$$\underline{\lambda}^{\mathrm{T}} \left(\mathcal{N}^{\mathrm{T}} \mathbf{P} \mathcal{N} \right) \underline{\lambda} = 0 \tag{3.7}$$

where $\underline{\lambda}$ is the weighting factor of the null space basis, $\mathcal{N}$ is the null space basis of the Jacobian matrix, and $\mathbf{P}$ is the projection matrix representing the projections of the singular angular momentum vectors onto the singular direction.

When $\mathbf{P}$ is definite (its eigenvalues are either positive or negative), no null motion is possible at this singular configuration[2] and the quadratic form in Eq.(3.7) has the form of an ellipsoid. Hence this kind of internal singularity is referred to as elliptic singularity[1,2].

On the other hand, when $\mathbf{P}$ is indefinite (its eigenvalues are both positive and negative) or semi-definite (at least one of its eigenvalues is zero), null motion can be used to steer the system away from singular configurations[2] and the quadratic form in Eq.(3.7) has the form of a hyperboloid. Hence this type of internal singularity is referred to as hyperbolic singularity[1,2].

IV. INVERSE KINEMATICS AND AVOIDANCE ALGORITHMS

1. Pseudoinverse Solution

The kinematics of a SCMG (RM) system is a nonlinear and pointwise mapping $f : \Re^n \rightarrow \Re^m$ such that closed-form inverse cannot be obtained. Hence the solution (inverse) is generally obtained using the resolved motion rate control[11]. The problem is formulated as

$$\underline{\tau} = \mathbf{J}\dot{\underline{\sigma}} \tag{4.1}$$

and the inverse kinematics can be expressed as

$$\dot{\underline{\sigma}} = \mathbf{J}^{+}\underline{\tau} + \left(\mathbf{I} - \mathbf{J}^{+}\mathbf{J}\right)\underline{v}(t) \tag{4.2a}$$

for redundant systems ($m < n$), or

$$\dot{\underline{\sigma}} = \mathbf{J}^{-1}\underline{\tau} \tag{4.2b}$$

for non-redundant systems ($m = n$). In Eq.(4.2a) $\mathbf{J}^{+}$ denotes the Moore-Penrose pseudoinverse[9] of $\mathbf{J}$ and $\underline{v}(t)$ denotes an arbitrary time-varying vector to provide singularity avoidance.

The numerical values of $\underline{v}(t)$ depend on how close the system is to being singular. The closer the system is to being singular, the higher the numerical values of $\underline{v}(t)$ are to provide singularity avoidance. The closeness of the system to being singular is often referred to as the singularity measure, or sometimes as the manipulatability index[11], which is expressed as

$$\mathcal{M} \triangleq \sqrt{\det\left(\mathbf{J}\mathbf{J}^{\mathrm{T}}\right)} \tag{4.3}$$

The system reaches singular configuration when $\mathcal{M}$ vanishes; $\left(\mathbf{J}\mathbf{J}^{\mathrm{T}}\right)^{-1}$, and hence $\mathbf{J}^{+}$, is not defined due to $\mathbf{J}$ being rank deficient. Thus $\underline{v}(t)$ is usually chosen such that $\mathcal{M}$ is locally maximized.

The disadvantages of Eq.(4.2a) are: (a) Existence of rank preservation of the Jacobian matrix is not guaranteed, (b) Extensive and costly computational effort is required to obtain a solution, (c) Singularity problems cannot be avoided successfully as demonstrated in Ref.2, and (d) Feasible solutions cannot be obtained in the neighborhoods of singular configurations because gimbal (linkage) rates are limited by some hardware constraints.

2. Singularity Robust Inverse

Nakamura and Hanafusa[7] presents a singularity robust (SR) inverse to solve the inverse kinematics problem in RM systems. This method was shown to work as well in the SCMG systems[2]. The singularity robustness is defined as a property of inverse kinematics that can provide continuous and feasible solutions for all gimbal (linkage) configurations (including the singular configurations).

The SR inverse is the solution of the unconstrained minimization problem:

$$\min_{\underline{\dot{\sigma}}} \quad \underline{\dot{\sigma}}^{\mathrm{T}}\underline{\dot{\sigma}} + \left(\underline{\tau} - \mathbf{J}\underline{\dot{\sigma}}\right)^{\mathrm{T}}\left(\underline{\tau} - \mathbf{J}\underline{\dot{\sigma}}\right) \tag{4.4}$$

The solution of Eq.(4.4) can be written as

$$\underline{\dot{\sigma}} = \mathbf{J}^{*}\underline{\tau} \tag{4.5a}$$

where

$$\mathbf{J}^{*} \triangleq \mathbf{J}^{\mathrm{T}}\left(\mathbf{J}\mathbf{J}^{\mathrm{T}} + \alpha\mathbf{I}\right)^{-1} \tag{4.5b}$$

is the SR inverse of the Jacobian matrix which is shown in Ref.11 to belong to the orthogonal complement of the redundant space. Alternatively the SR inverse, $\mathbf{J}^*$, can be computed using the singular value decomposition[2,7,11] of the Jacobian matrix

$$\mathbf{J}^* = \mathbf{V}\Sigma^*\mathbf{U}^{\mathrm{T}} \tag{4.6}$$

where

$$\mathbf{U} \in \Re^{m\times m} \quad \text{and} \quad \mathbf{V} \in \Re^{n\times n} \text{ are orthonormal matrices}$$

$$\Sigma^* = \begin{pmatrix} \Sigma_{\mathrm{J2}} & 0 \\ 0 & 0 \end{pmatrix} \in \Re^{n\times m}$$

$$\Sigma_{\mathrm{J2}} \triangleq \mathrm{diag}\left(\frac{\sigma_i}{\sigma_i^2 + k}\right) \in \Re^{l\times l}$$

If the system is singular, the SR inverse results in the gimbal (linkage) lock phenomenon: the gimbals (linkages) are "locked" in the singular configuration[2,10] and extra effort is required to escape from the singular configurations.

3. Extended Jacobian Technique

The extended Jacobian technique is proposed by Baillieul[3] as a kinematic programming alternative to solve the inverse kinematics in RM systems. This technique takes advantage of the redundancy in the system by imposing conditions that the gimbal (linkage) configurations optimize (at least locally) some objective function $g(\sigma)$ which could be the singularity measure or manipulatability index.

The kinematics of a SCMG (RM) system can be represented as

$$\underline{x} = \underline{F}(\sigma) \tag{4.7}$$

where $\underline{x}$ denotes angular momentum (trajectory) of SCMG (RM) systems and σ denotes gimbal (linkage) configurations. Let the Jacobian matrix be defined as

$$\mathbf{J} \triangleq \frac{\partial F}{\partial \underline{\sigma}} \tag{4.8}$$

and $\mathcal{N}$ denote the null space basis of the Jacobian matrix which can be calculated using *generalized cross product* [1,2] or QR decomposition[9] of $\mathbf{J}$.

The condition for optimizing the objective function $g(\sigma)$ is given by[7]

$$G(\sigma) = 0 \tag{4.9}$$

where

$$G(\sigma) \triangleq \frac{\partial g}{\partial \underline{\sigma}}(\sigma) \cdot \mathcal{N}$$

If some gimbal (linkage) configurations satisfy Eq.(4.7) while, at the same time, optimizing $g(\sigma)$, then

$$\begin{Bmatrix} \underline{F}(\sigma(t)) \\ G(\sigma(t)) \end{Bmatrix} = \begin{Bmatrix} \underline{x}(t) \\ 0 \end{Bmatrix} \tag{4.10}$$

Thus the differential relationships for Eq.(4.10) can be written as

$$\begin{pmatrix} \mathbf{J} \\ \frac{\partial G}{\partial \underline{\sigma}} \end{pmatrix} \dot{\underline{\sigma}}(t) = \begin{Bmatrix} \dot{\underline{x}}(t) \\ 0 \end{Bmatrix} \tag{4.11}$$

where $\frac{\partial G}{\partial \underline{\sigma}}$ is the gradient of $G(\sigma)$ with respect to $\underline{\sigma}$. Thus

$$\begin{pmatrix} \mathbf{J} \\ \frac{\partial G}{\partial \underline{\sigma}} \end{pmatrix} \tag{4.12}$$

is a square matrix and is referred to as the extended Jacobian, $\mathbf{J}_e$. Therefore, provided that $\mathbf{J}_e$ is not singular, the solution to the inverse kinematics problem is given by

$$\dot{\underline{\sigma}}(t) = \mathbf{J}_e^{-1} \begin{Bmatrix} \dot{\underline{x}}(t) \\ 0 \end{Bmatrix} \tag{4.13}$$

The extended Jacobian, $\mathbf{J}_e$, defined in Eq.(4.12) has some drawback: there exist some gimbal (linkage) configurations, $\underline{\sigma}_s$, such that $\mathbf{J}_e(\underline{\sigma}_s)$ is singular but $\mathbf{J}(\underline{\sigma}_s)$ has full rank. Thus the system now has more than 2^n singular configurations for a given singular direction in $\Re^m$ which should be avoided by this technique.

V. PROPOSED SINGULARITY AVOIDANCE ALGORITHM

The inverse kinematics and singularity avoidance methods presented in Chapter IV have several drawbacks that leave room for improvement. The pseudoinverse solution cannot avoid elliptic singularities successfully and require extensive and costly computational task. The singularity robust inverse can provide solution in the neighborhoods of singularities albeit approximate. However, the solution might result in the gimbal (linkage) lock phenomenon. The extended Jacobian technique can eliminate the avoidable singularities, but it introduces additional singular configurations other than those due to kinematics, i.e. the solution cannot be obtained even if the gimbal (linkage) configurations are not kinematically singular. This chapter presents a proposed algorithm which is expected to provide some improvements for the inverse kinematics and singularity avoidance algorithms. The proposed algorithm is similar to the extended Jacobian technique and pseudoinverse solution.

The kinematics problem is generally formulated as in Eq.(4.7) and the differential relationships can be expressed as

$$\underline{\dot{x}} = \mathbf{J}\underline{\dot{\sigma}} \tag{5.1}$$

where $\mathbf{J}$ is the Jacobian matrix defined as

$$\mathbf{J} \triangleq \frac{\partial \underline{F}}{\partial \underline{\sigma}} \tag{5.2}$$

The inverse kinematics problem will be solved using the following algorithm which will also provide singularity avoidance.

PROPOSITION

Assume that at $t_i \in [t_0, t_f)$ Rank$[\mathbf{J}(t_i)] = m$ and let $\mathcal{N}$ be the null space basis of $\mathbf{J}$ $(\in \Re^n)$. Augmenting (5.1) with $\mathcal{N}^{\mathrm{T}}\dot{\underline{\sigma}} = \psi$ yields

$$\mathbf{J}_e\dot{\underline{\sigma}} = \underline{x}_e \tag{5.3a}$$

where $\mathbf{J}_e \in \Re^{n\times n}$ is the extended Jacobian defined as

$$\mathbf{J}_e \triangleq \begin{pmatrix} \mathbf{J} \\ \mathcal{N}^{\mathrm{T}} \end{pmatrix} \tag{5.3b}$$

and $\underline{x}_e$ is the extended operational task defined as

$$\underline{x}_e \triangleq \begin{Bmatrix} \dot{\underline{x}} \\ \psi \end{Bmatrix} \tag{5.3b}$$

Hence the solution of the inverse kinematics problem is given by

$$\dot{\underline{\sigma}} = \mathbf{J}_e^{-1}\underline{x}_e \tag{5.4}$$

which is equivalent to (4.2a) and similar to Eq.(4.13).

PROOF

A pseudoinverse of a nonsingular square matrix is equal to the regular inverse. If rank$(\mathbf{J}) = m$, then $\mathbf{J}_e$ is a nonsingular square matrix. Hence

$$\begin{aligned}
\mathbf{J}_e^{-1} &= \mathbf{J}_e^{+} \\
&= \begin{pmatrix} \mathbf{J}^{\mathrm{T}} & \mathcal{N} \end{pmatrix} \left[\begin{pmatrix} \mathbf{J} \\ \mathcal{N}^{\mathrm{T}} \end{pmatrix} \begin{pmatrix} \mathbf{J}^{\mathrm{T}} & \mathcal{N} \end{pmatrix} \right]^{-1} \\
&= \begin{pmatrix} \mathbf{J}^{\mathrm{T}} & \mathcal{N} \end{pmatrix} \begin{pmatrix} \left(\mathbf{J}\mathbf{J}^{\mathrm{T}}\right)^{-1} & 0 \\ 0 & 1 \end{pmatrix} \\
&= \begin{pmatrix} \mathbf{J}^{+} & \mathcal{N} \end{pmatrix}
\end{aligned}$$

Hence Eq.(5.4) can be rewritten as

$$\dot{\underline{\sigma}} = \mathbf{J}^{+}\dot{\underline{x}} + \psi\mathcal{N}$$

which is equivalent to Eq.(4.2a) and similar to Eq.(4.13) ∎

COROLLARY

The manipulatability index or singularity measure is defined as

$$\mathcal{M}_e = \det(\mathbf{J}_e)$$

which is equivalent to Eq.(4.3).

In Eqs.(5.3–4), ψ is a parameter playing a similar role as $\underline{v}(t)$ in Eq.(4.7). The proposed algorithm has a geometrical interpretation: "scaled" projection of the solution, $\underline{\dot{\sigma}}$, onto the null space direction (basis) of the Jacobian matrix. In general, ψ is a function of time and is problem-dependent, and its form is given by:

$$\psi = C \cdot \det(\mathbf{J}_e) \cdot \text{norm}(\underline{\dot{\sigma}}_{\text{MP}})^p \tag{5.5}$$

where $\underline{\dot{\sigma}}_{\text{MP}}$ denotes the particular solution of the Moore-Penrose pseudoinverse and C and p are problem-dependent constants.

The proposed algorithm is applied to solve two SCMG singularity avoidance problems. In the first simulation, the constant unit torque ($\tau = \{1\ 0\ 0\}^{\text{T}}$) along the $\mathcal{V}_1$ axis is requested. This torque forces the system to go towards both internal and saturation singular configurations. In the second simulation, the torque request is defined as

$$\underline{\tau} = \begin{cases} \{0.7071 \quad 0.7071 \quad 0\}^{\text{T}} & , \ t < 0.83 \text{ (s)} \\ \{-0.7071 \quad 0.7071 \quad 0\}^{\text{T}} & , \ 0.83 \leq t < 4.0 \text{ (s)} \end{cases}$$

Each gimbal in both simulations has an angular momentum, h, of 1.0 kg-m^2/s.

The CMG dynamics are integrated using the seventh-eighth order Runge-Kutta-Fehlberg integrator on MATLAB with a tolerance value of 10^{-6}. The magnitude of the gimbal rate vector is limited such that $|\underline{\dot{\sigma}}|_2 \leq 4$. The parameters in Eq.(5.5) used for the first simulation are $C = 1.25, p = 1.5$, and those for the second simulation are $C = p = 1$.

The results of the simulations show that the proposed algorithm has successfully avoided the elliptic singular configurations (Figs.7 and Figs.8); the algorithm generates singularity-free gimbal configurations until saturation singular configurations are reached. This algorithm shows its superiority over the pseudoinverse and singularity robust inverse solutions presented in Ref.2.

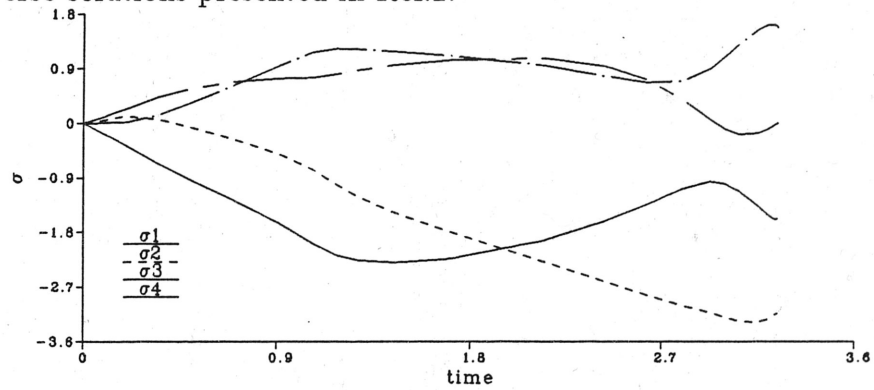

(a)

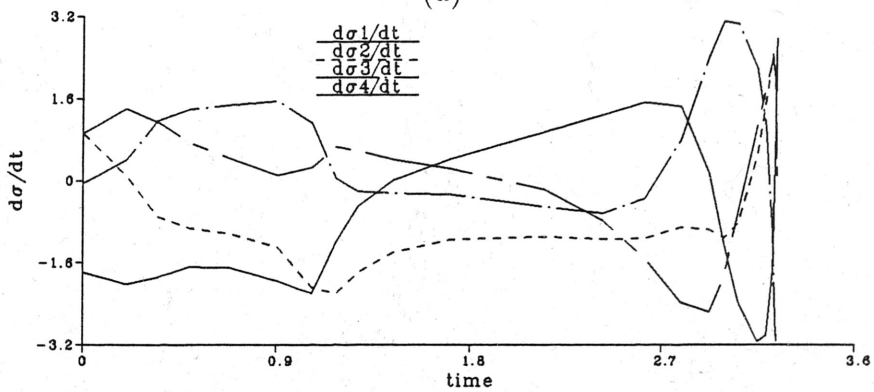

(b)

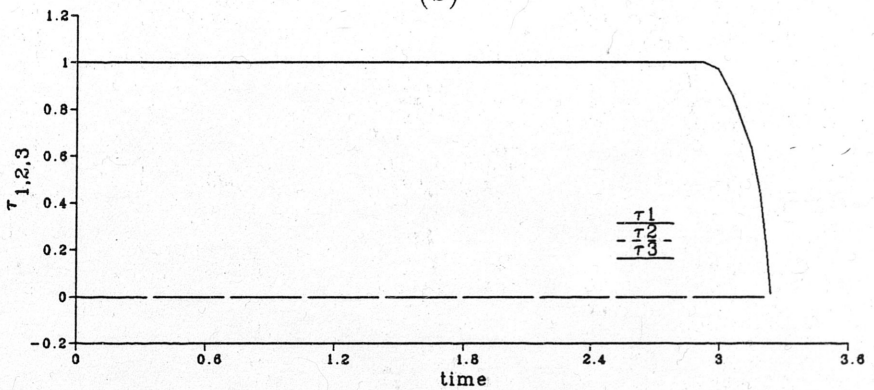

(c)

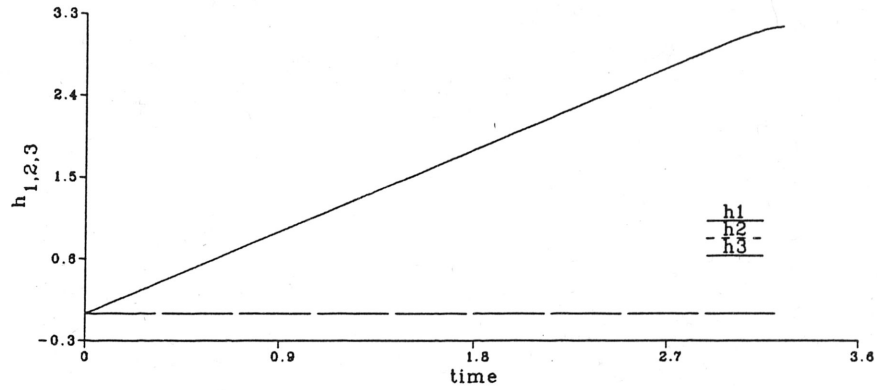

(d)

Figure 7 Results of simulation I: (a) Gimbal angles (rad), (b) Gimbal rates (rad/s), (c) Output torque (N-m), (d) Gimbal angular momentum (kg-m^2/s).

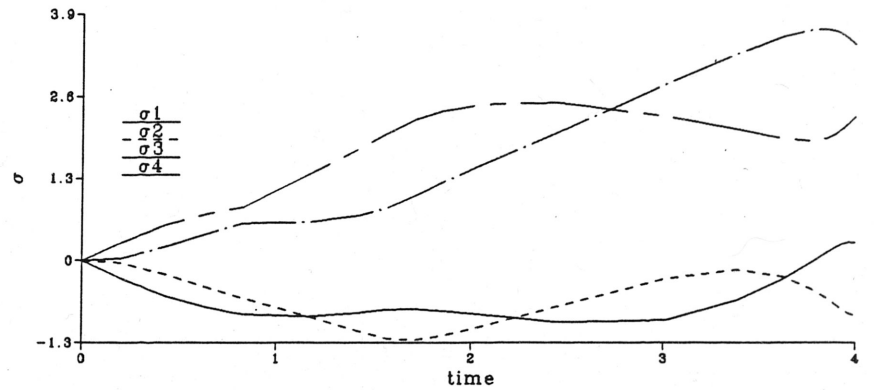

(a)

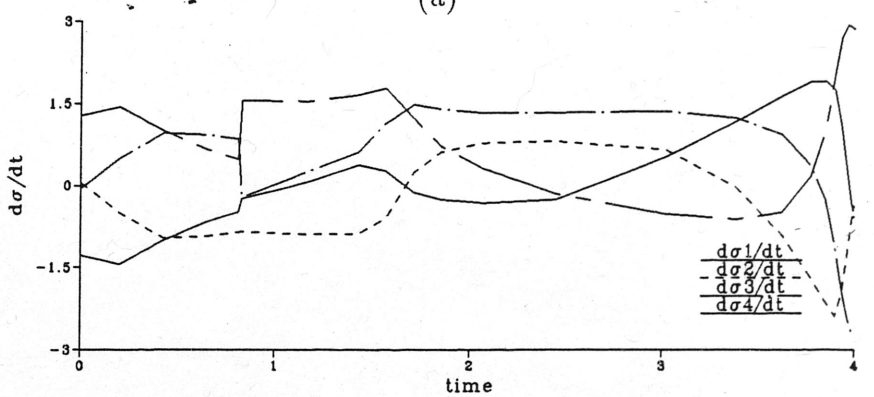

(b)

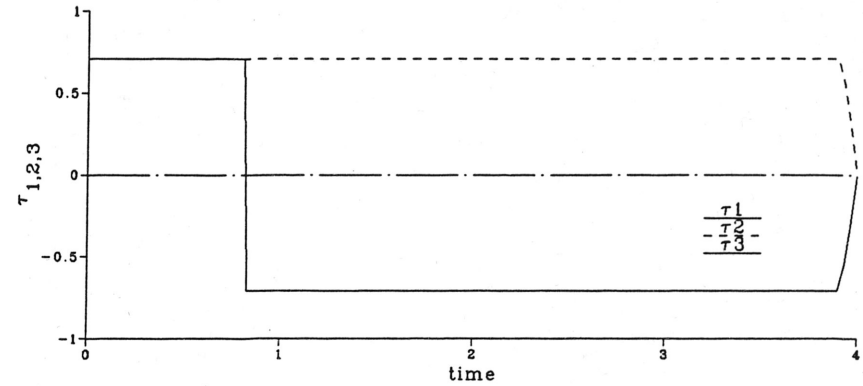

(c)

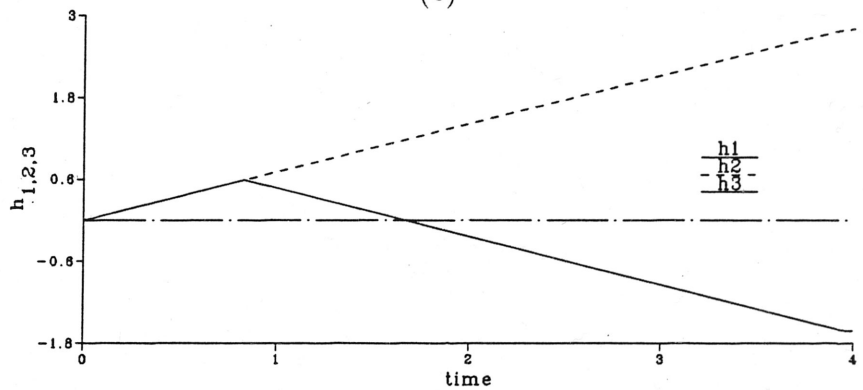

(d)

Figure 8 Results of simulation II: (a) Gimbal angles (rad), (b) Gimbal rates (rad/s), (c) Output torque (N-m), (d) Gimbal angular momentum (kg-m^2/s).

VI. FEEDBACK CONTROL IN SPACECRAFT DYNAMICS

1. Introduction

Attitude stabilization and control systems are very important parts of spacecraft design. Many spacecraft must maintain their attitude within a fine tolerance and point in the right direction. For example, the Hubble Space Telescope must point its sensors towards certain stars very accurately and the Phase-1 space station must maintain its attitude within $\pm 5^{\circ}$ of local vertical local horizontal (LVLH)[12].

Some spacecraft are designed to perform rapid large angle maneuvering and target tracking. Such spacecraft require nonlinear control laws and high authority actuators to generate required torques to perform the tasks. Single gimbal control moment gyroscopes are suitable for use in such application as they can provide torque amplification and generate continuous torque to perform rapid slew maneuvering and precision pointing/target tracking.

This chapter shows two examples of application of SCMGs in spacecraft maneuvers. The proposed algorithm is applied to generate the required torque and provide singularity avoidance (obtain singularity-free gimbal configurations). In the first simulation, a rest-to-rest spacecraft reorientation maneuver is performed, while a motion-to-rest spacecraft maneuver is performed in the second.

2. Spacecraft Attitude Dynamics

The spacecraft attitude is represented by a set of Euler parameters which describe the relative rotation of the vehicle frame with respect to the inertial frame of reference.

When orbital motion is ignored, the time derivative of the Euler parameters is related to the vehicle angular velocity by[10]

$$\dot{\underline{\beta}} = \frac{1}{2}\mathbf{G}_\beta \underline{\omega} \tag{6.1}$$

where $\underline{\beta} = \{\beta_0\ \beta_1\ \beta_2\ \beta_3\}^{\mathrm{T}}$ and $\underline{\omega} = \{\omega_1\ \omega_2\ \omega_3\}^{\mathrm{T}}$ are the Euler parameters and vehicle angular velocity, respectively, and $\mathbf{G}_\beta$ is given by

$$\mathbf{G}_\beta \triangleq \begin{pmatrix} -\beta_1 & -\beta_2 & -\beta_3 \\ \beta_0 & -\beta_3 & \beta_2 \\ \beta_3 & \beta_0 & -\beta_1 \\ -\beta_2 & \beta_1 & \beta_0 \end{pmatrix}$$

The spacecraft total angular momentum can be written as

$$\underline{H} = \mathbf{I}\underline{\omega} + \underline{h}_{\mathrm{CMG}} \tag{6.2}$$

where $\mathbf{I}$ is the inertia of the spacecraft. The time derivative of the angular momentum is derived using the Newton-Euler principle[10] as

$$\underline{L}_c = \frac{d\underline{H}}{dt} = \mathbf{I}\dot{\underline{\omega}} + \underline{\omega} \times \mathbf{I}\underline{\omega} + \dot{\underline{h}}_{\mathrm{CMG}} \tag{6.3a}$$

or, in the absence of external torques, $\underline{L}_c = \underline{0}$, Eq.(6.3a) can be rewritten as

$$\dot{\underline{\omega}} = \mathbf{I}^{-1}\left[-\underline{\omega} \times (\mathbf{I}\underline{\omega} + \underline{h}_{\mathrm{CMG}}) - \dot{\underline{h}}_{\mathrm{CMG}}\right] \tag{6.3b}$$

The effect of gimbal and transverse inertias is small compared to that of the spacecraft, thus the SCMG inertia terms are neglected in the analysis[10].

3. Feedback Control of Spacecraft Maneuvers

A feedback control law is a relationship between the required torque and the instantaneous and target states. The control design is based on Liapunov's second method[10]. which guarantees global asymptotic stability of the control system as long as no singularities are encountered in the SCMG system.

Without loss of generality, the desired final attitude is assumed as $\underline{\beta}_f = \{1\ 0\ 0\ 0\}^T$. The spacecraft initial angular velocity is $\underline{\omega}_o$ while its final angular velocity is zero.The Liapunov function is defined as

$$V \triangleq (\beta_0 - 1)^2 + \beta_1^2 + \beta_2^2 + \beta_3^2 + \frac{1}{2}\underline{\omega}^T \mathbf{I} \underline{\omega} \tag{6.4}$$

which is the deviation squared of the instantaneous states from the target states. It is necessary, for stability of the feedback control system, that V be a monotonically decreasing function; therefore, its time derivative must be negative throughout the maneuver. It is sufficient, for $\dot{V} < 0$, that[10]

$$\underline{\dot{h}}_{\text{CMG}} = \mathbf{J}\underline{\dot{\sigma}} = k\hat{\beta} + \mathbf{K}\underline{\omega} \tag{6.5}$$

where $\hat{\beta} \triangleq \{\beta_1\ \beta_2\ \beta_3\}^T$, k is a positive constant, and $\mathbf{K}$ is a positive definite gain matrix.

4. Simulations

The proposed algorithm is applied to solve singularity avoidance problems in spacecraft attitude control systems using SCMG. The spacecraft data in the simulation are taken from Ref.10. Torque demands are generated using feedback control law based on the Liapunov's stability theorem[10].

The first simulation is a rest-to-rest spacecraft reorientation maneuver. The initial attitude of the spacecraft is defined as $\underline{\beta}_o = \{0.7071\ 0.7071\ 0\ 0\}^T$ while its initial angular velocity is zero. Each gimbal in the SCMG system has an angular momentum, h, of 1.15 kg-m^2/s. The second simulation is a motion-to-rest spacecraft maneuver. The initial attitude of the spacecraft is defined as $\underline{\beta}_o = \{0.7071\ 0.7071\ 0\ 0\}^T$ while its initial angular velocity is defined as $\underline{\omega}_o = \{-01\ -05\ 001\}^T$. Each gimbal in the SCMG system has an angular momentum, h, of 2.1 kg-m^2/s.

The system equations: Eqs.(6.1),(6.3b),(6.5) are integrated using a seventh-eighth order Runge-Kutta-Fehlberg integrator on MATLAB with a tolerance value of 10^{-6}. The magnitude of the gimbal rate vector is limited such that $|\underline{\dot{\alpha}}|_2 \leq 4$. The parameters in Eq.(5.5) used for the first simulation are $C = p = 1$, and those for the second simulation are $C = 1, p = 2$. The results of the simulations show the present algorithm generates singularity-free gimbal configurations during the maneuvers in these particular examples (Figs.9 and Figs.10).

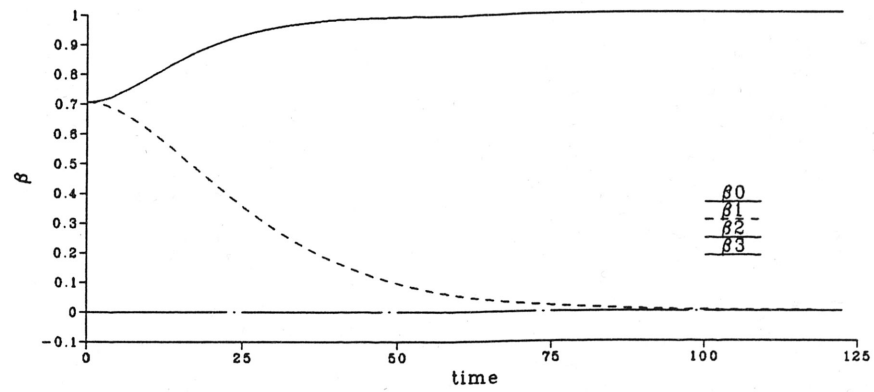

(a)

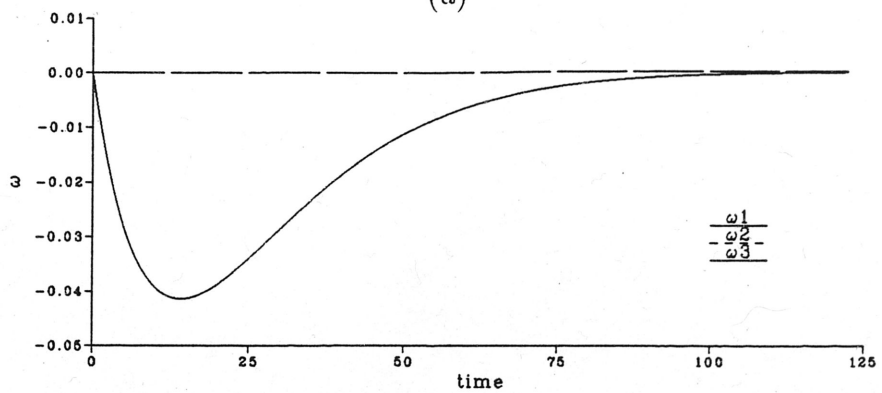

(b)

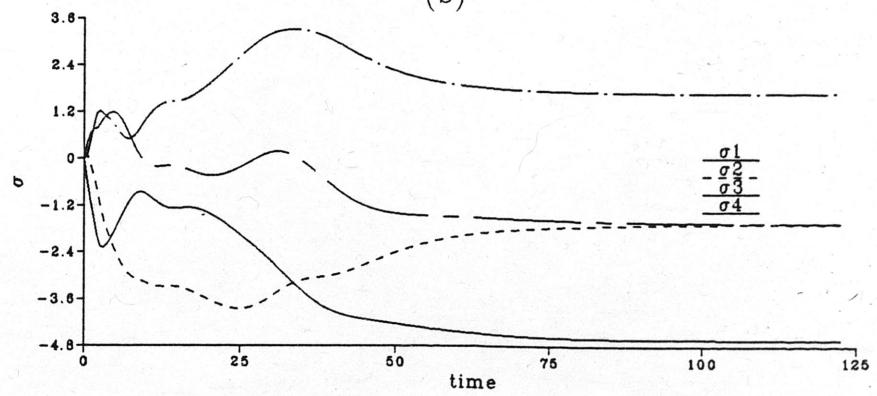

(c)

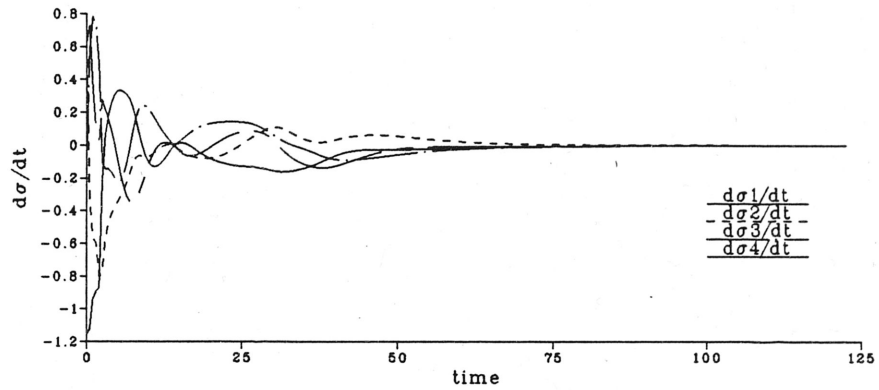
0.8
0.6
0.4
0.2
0
-0.2
-0.4
-0.6
-0.8
-1
-1.2
dσ/dt
0
25
50
75
100
125
time
dσ1/dt
dσ2/dt
dσ3/dt
dσ4/dt

(d)

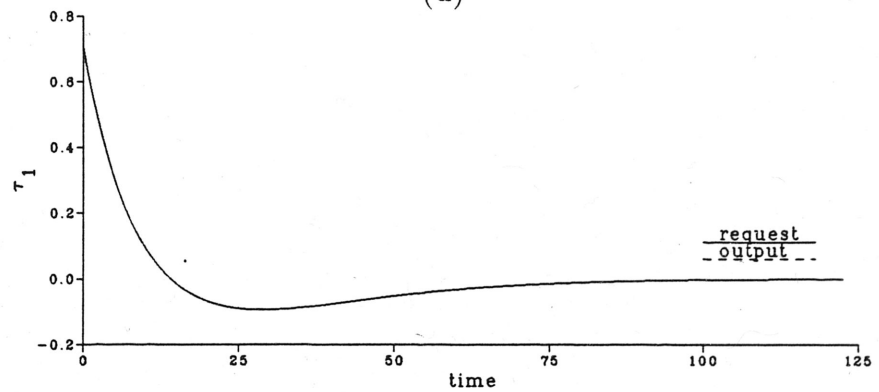
0.8
0.6
0.4
0.2
0.0
-0.2
τ_1
0
25
50
75
100
125
time
request
output

(e)

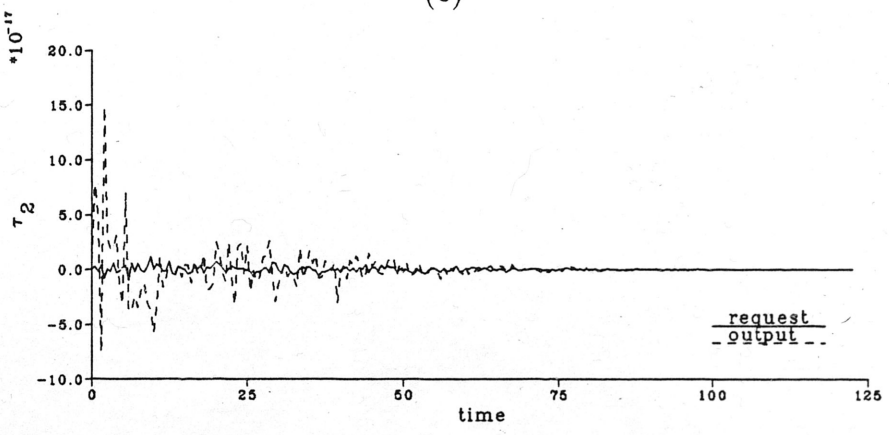
*10⁻¹⁷
20.0
15.0
10.0
5.0
0.0
-5.0
-10.0
τ_2
0
25
50
75
100
125
time
request
output

(f)

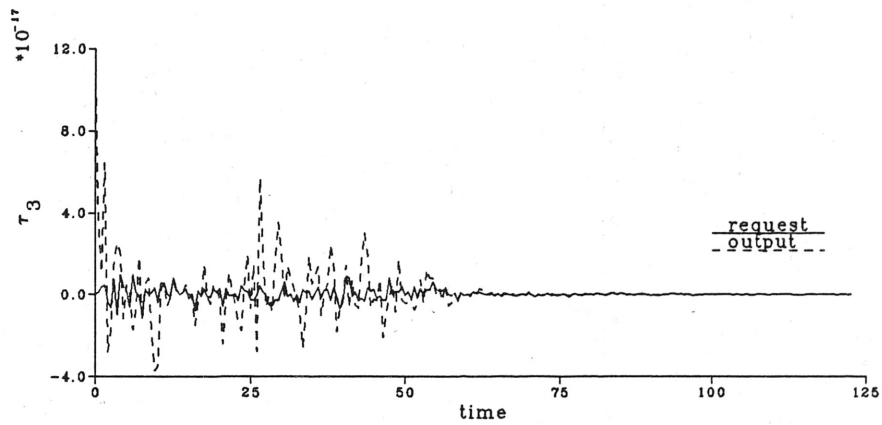

(g)

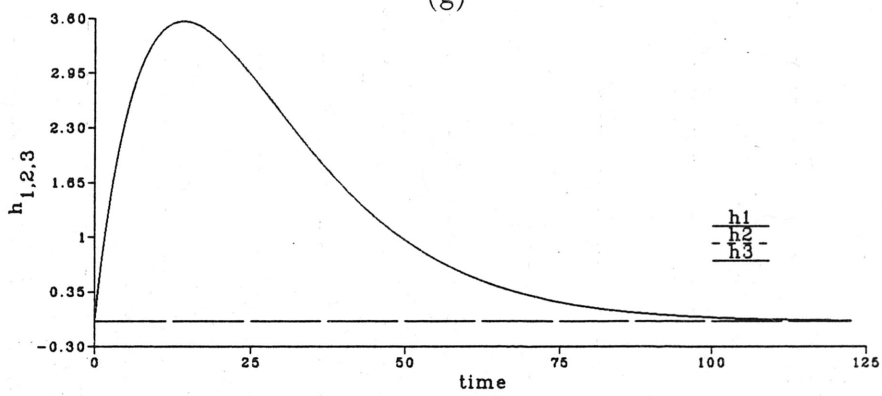

(h)

Figure 9 Results of the rest-to-rest spacecraft reorientation maneuver: (a) Euler parameters, (b) Spacecraft angular velocity (rad/s), (c) Gimbal angles (rad), (d) Gimbal rates (rad/s), (e) Requested v. output torques in the $\mathcal{V}_1$ axis (N-m), (f) Requested v. output torques in the $\mathcal{V}_2$ axis (N-m), (g) Requested v. output torques in the $\mathcal{V}_3$ axis (N-m), (h) Gimbal angular momentum (kg-m^2/s).

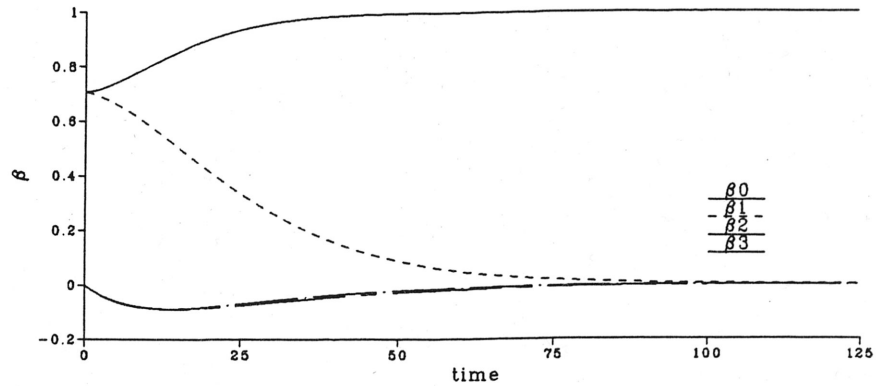

(a)

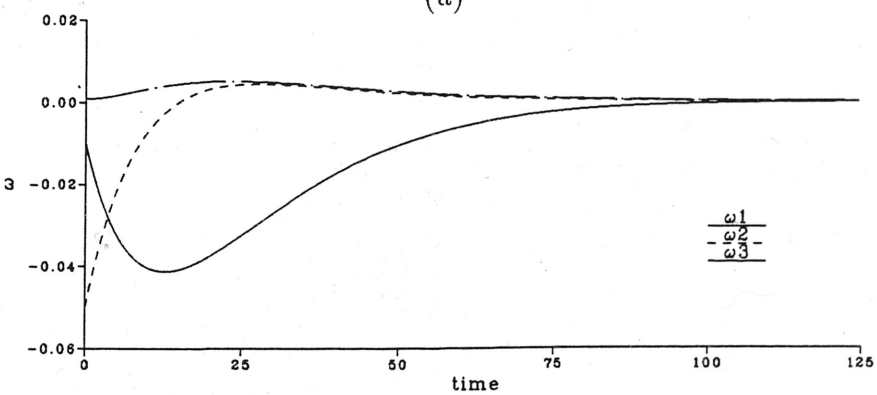

(b)

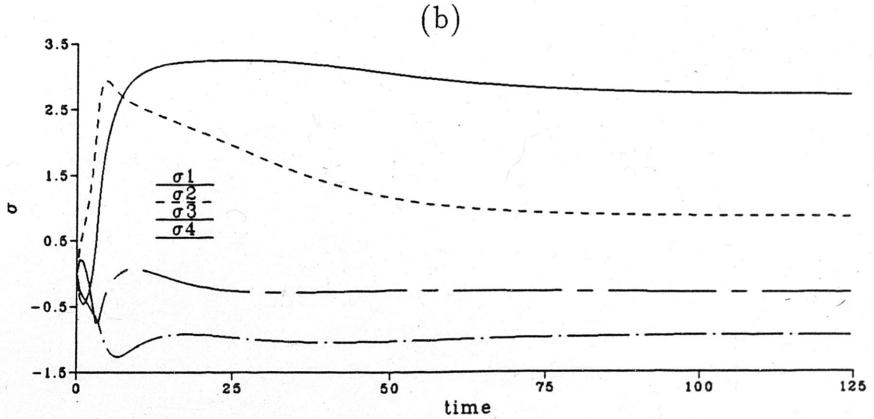

(c)

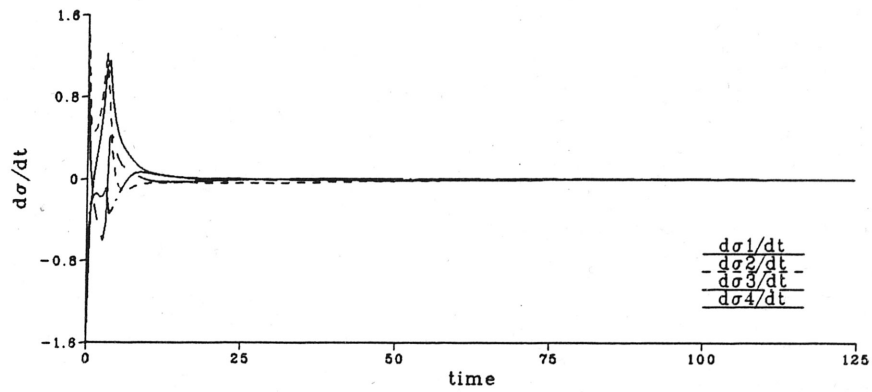
1.6
0.8
0
-0.8
-1.6
dσ/dt
0
25
50
75
100
125
time
dσ1/dt
dσ2/dt
dσ3/dt
dσ4/dt

(d)

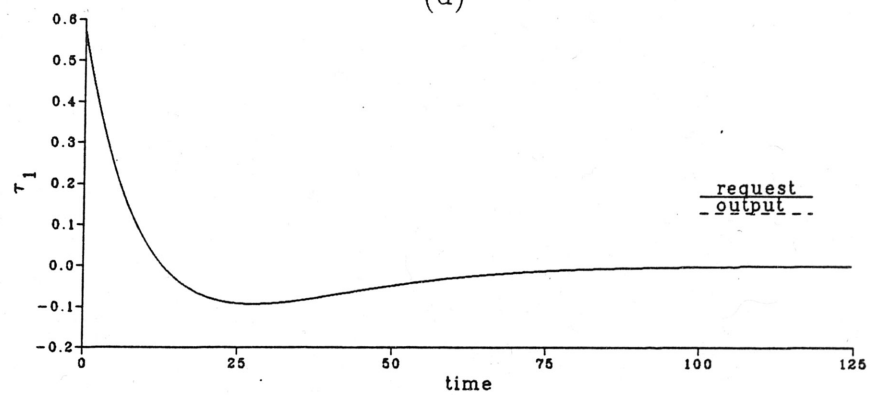
0.6
0.5
0.4
0.3
0.2
0.1
0.0
-0.1
-0.2
τ1
0
25
50
75
100
125
time
request
output

(e)

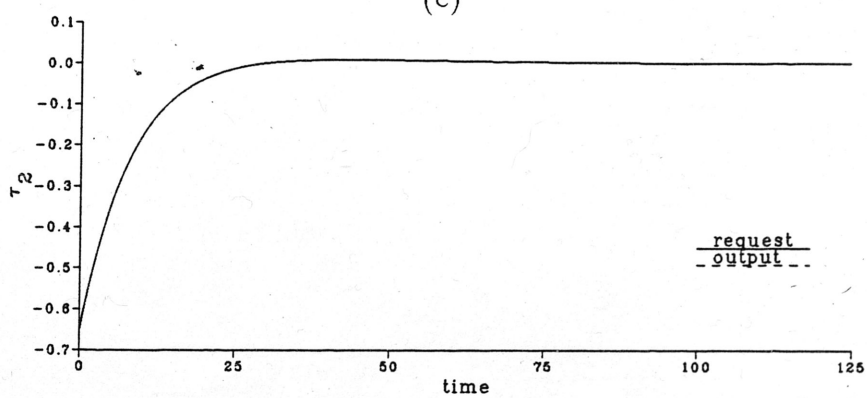
0.1
0.0
-0.1
-0.2
-0.3
-0.4
-0.5
-0.6
-0.7
τ2
0
25
50
75
100
125
time
request
output

(f)

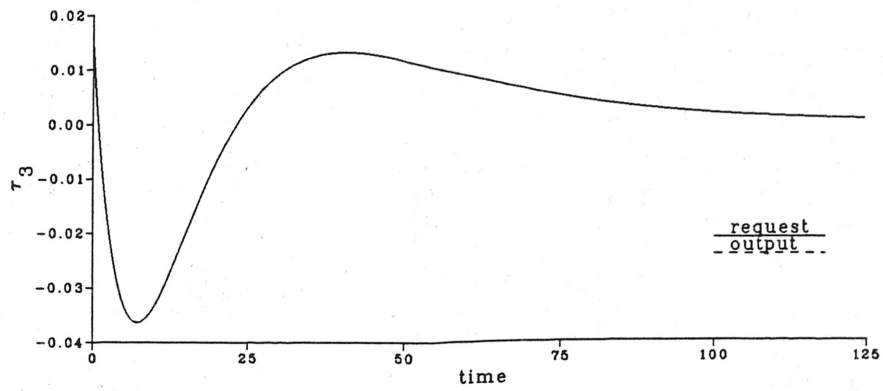

(g)

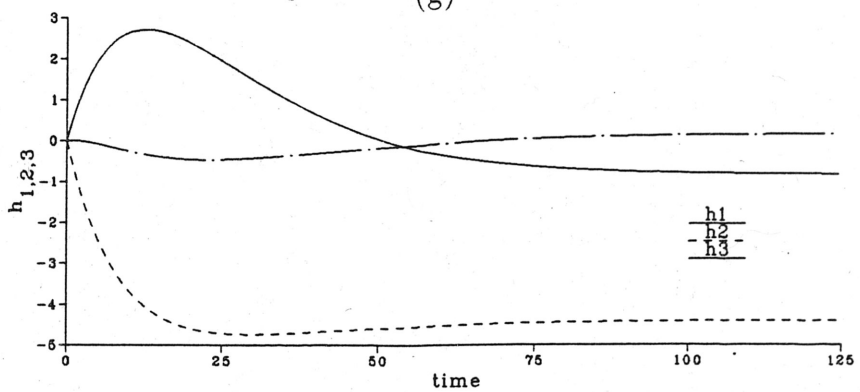

(h)

Figure 10 Results of the motion-to-rest spacecraft maneuver: (a) Euler parameters, (b) Spacecraft angular velocity (rad/s), (c) Gimbal angles (rad), (d) Gimbal rates (rad/s), (e) Requested v. output torques in the $\mathcal{V}_1$ axis (N-m), (f) Requested v. output torques in the $\mathcal{V}_2$ axis (N-m), (g) Requested v. output torques in the $\mathcal{V}_3$ axis (N-m), (h) Gimbal angular momentum (kg-m^2/s).

VII. CONCLUSIONS AND RECOMMENDATIONS

The proposed algorithm can avoid singularities by steering the system away from singular configurations. Choice of a proper value of ψ generates a singularity free path (avoids internal singularities). Further study needs to be conducted to obtain a systematic way of choosing the proper value of ψ. Alternatively, optimal control theory may be applied to generate singularity free path in both SCMG and RM systems. This is recommended as a topic of future research.

REFERENCES

1. Margulies G., Aubrun J., "Geometric Theory of Single Gimbal Control Moment Gyro Systems," *Journal of Astronautical Sciences*, Vol. XXVI, No. 2, April–June 1978, pp. 159–191.

2. Bedrossian N., "Steering Law Design for Redundant Single Gimbal Control Moment Gyro Systems," M.S. Thesis, Massachusetts Institute of Technology, Mechanical Eng., Aug. 1987.

3. Baillieul J., "Kinematic Programming Alternatives for Redundant Manipulators," *IEEE Intl. Conf. on Robotics and Automation*, St. Louis MO, March 1985, pp. 722–728.

4. Mayorga R., Wong A., "A Singularities Prevention Approach for Redundant Robot Manipulators," *IEEE Intl. Conf. on Robotics and Automation*, Cincinnati OH, May 1990, pp. 812–817.

5. Nenchev D., "Redundancy Resolution through Local Optimization: A Review," *Journal of Robotic Systems*, Vol. 6.6, Dec. 1989.

6. Cornick D.E., "Singularity Avoidance Control Laws for Single Gimbal Control Moment Gyros," *AIAA Guidance and Control Conf.*, Boulder CO, *AIAA* paper 79-1698, Aug. 1979.

7. Nakamura Y., Hanafusa H., "Inverse Kinematic Solutions with Singularity Robustness for Robot Manipulator Control," *Journal of Dynamic Systems, Measurement, and Control*, Vol. 108, Sept. 1986, pp. 163–171.

8. Vadali S., Oh H., Walker S., "Preferred Gimbal Angles for Single Gimbal Control Moment Gyros," *AIAA Navigation, Guidance and Control Conf.*, Boston MA, *AIAA* paper 89-3477, Aug. 1989.

9. Golub G., Van Loan C., *Matrix Computation*, 2nd Ed., The Johns Hopkins University Press, Baltimore MD, 1989.

10. Oh H., "Feedback Control and Steering Laws for Spacecraft Using Single Gimbal Control Moment Gyros," M.S. Thesis, Texas A&M University, Aerospace Eng., Dec. 1988.

11. Nakamura Y., *Advanced Robotics: Redundancy and Optimization*, Addison Wesley, Reading MA, 1991.

12. Vadali S., Oh H., "Space Station Attitude Control and Momentum Management: A Nonlinear Look," *AIAA Guidance, Control, and Navigation Conf.*, Portland OR, *AIAA* paper 90-3353, Aug. 1990.